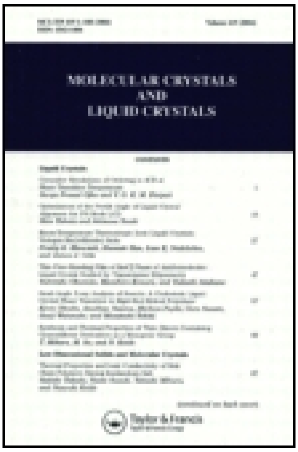

Molecular Crystals and Liquid Crystals Science and Technology. Section A. Molecular Crystals and Liquid Crystals

Publication details, including instructions for authors and subscription information:
http://www.tandfonline.com/loi/gmcl19

Spin Dynamics of Photoexcitations in C_{60} and C_{60}

Xing Wei [a] & Z. Valy Vardeny [a]

[a] Department of Physics, University of Utah, Salt Lake City, Utah, 84112, U.S.A.

To cite this article: Xing Wei & Z. Valy Vardeny (1994): Spin Dynamics of Photoexcitations in C_{60} and C_{60} , Molecular Crystals and Liquid Crystals Science and Technology. Section A. Molecular Crystals and Liquid Crystals, 256:1, 307-315

To link to this article: http://dx.doi.org/10.1080/10587259408039261

Mol. Cryst. Liq. Cryst. 1994, Vol. 256, pp. 307–315
Reprints available directly from the publisher
Photocopying permitted by license only

SPIN DYNAMICS OF PHOTOEXCITATIONS IN C_{60} AND C_{70}

XING WEI and Z. VALY VARDENY
Department of Physics, University of Utah, Salt Lake City, Utah 84112, U. S. A.

Abstract We have used absorption detected magnetic resonance (ADMR) spectroscopy to study the spin dynamics of spin 1/2 and spin 1 photoexcitations in C_{60} and C_{70}, in molecular and solid-state forms. In C_{60} molecules dispersed in polystyrene matrix (C_{60}:PS), two $S = 1$ powder patterns were observed at 4 K; they collapse towards the central $g \approx 2$ magnetic resonance line with increasing temperature. We fit the results with a model that relates the two observed triplets with two Jahn-Teller distortion levels, respectively, subject to a temperature dependent pseudo rotation dynamics. In C_{70}:PS, we found that a $S = 1/2$ signal, which is associated with existing radicals in the sample, accompany the $S = 1$ ADMR signal. In sublimed C_{60} and C_{70} films, in addition to the triplet excitations with a quenching ADMR signal, we found an enhancing spin 1/2 ADMR signal. We explain this feature as due to charge separation, which uniquely occurs in sublimed films with excitation above the respective C_{60} and C_{70} energy gap.

INTRODUCTION

All-carbon molecules, buckminsterfullerenes, in particular C_{60} and C_{70}, have recently attracted considerable theoretical and experimental interests[1]. Their high symmetric molecular structures (icosahedral symmetry in C_{60} and D_{5h} symmetry in C_{70}) make their excited electronic states subject to dynamic Jahn-Teller (JT) distortion[2]. Several theoretical calculations have been carried out to study the JT distortion energy[3], and induced pair binding energies of JT distortions in negatively charged C_{60}[4-5] and in the lowest excited singlet state of C_{60}[6]. Auerbach et al[7] pointed out the importance of the quantum interference effects (Berry phases) in the pseudorotations of the C_{60} JT distortion. Recent studies of C_{60} and C_{70} in solutions and polystyrene glasses using light induced ESR (LESR)[8] and optically detected magnetic resonance[9-10] have shown that the long lived photoexcitations in C_{60} and C_{70} molecules are triplet excitons. The manifestation of JT effects on the spin dynamics of these triplet excitons have also been discussed[11-12]. C_{60} and C_{70} can also form molecular type crystal through the weak intermolecular van der Waals forces. Recent photoemission and inverse-photoemission[13] and elipsometric spectra[14-15] of C_{60} and C_{70} films show that they are molecular semiconductors with bandgap of 2.3 and 1.25 eV, respectively. Compared to C_{60} molecules, photophysical studies of C_{60} films have revealed several unexpected phenomena. First, self-trapped (polaronic) excitons are generated at low temperatures[16]. Second, charge-carriers are also photogenerated; they give rise to photoconductivity (PC)[16-17], photovoltaic[19], and xerographic effects[20], all with action spectra similar to the optical absorption spectrum.

In this work we study the spin dynamics of photoexcitations C_{60} and C_{70} in polystyrene (PS) matrices and C_{60} and C_{70} films, using the technique of absorption detected magnetic resonance (ADMR)[21]. Our present studies of spin dynamics in C_{60} and C_{70} films provide a more complete identification of the primary and long-lived photoexcitations and their dynamics.

EXPERIMENTAL

The ADMR technique uses a cw pump beam (from an Ar^+ laser) and a probe beam (from a tungsten lamp) to constantly illuminate the sample, which is mounted in a high Q microwave cavity (at 3 GHz) equipped with optical windows, and a superconducting magnet producing a field H. Microwave resonant absorption, modulated usually at 500 Hz, leads to small changes, δT, in the probe transmission T. This δT is proportional to δn, the change in the photoexcitation density n produced by the pump. δn is induced by transitions in the microwave range that change spin-dependent recombination rates.

Purified C_{60} (with purity > 99.9%) and C_{70} (with purity > 98%) powders, from the MER corp, were mixed in a solution of degassed toluene/polystyrene, which was subsequently evaporated to form C_{60} and C_{70}:PS glasses. The sublimed C_{60} and C_{70} thin films were deposited at MER on quartz and sapphire substrates at 450°C at a rate of 1 Å/sec from purified C_{60} and C_{70} powders, respectively. The films' thickness was about 3000 Å as determined from the film absorption spectrum.

RESULTS AND DISCUSSION

Figure 1 shows the ADMR spectra of C_{60}:PS glass at various temperatures, taken at a constant probe photon energy of 1.65 eV, which is the peak of the triplet-triplet photoinduced absorption (PA) band in C_{60}[22-23]. At 2K, the ADMR spectrum shows a 250 Gauss wide triplet powder pattern around $g \approx 2$ (1071 Gauss) with $\delta n/n = -6\times10^{-3}$.

The powder pattern contains four singularities and can be well fit[24] using $D = 0.0114\text{cm}^{-1}$ and $E = 0$. That $E = 0$ indicates that the triplet state is axially symmetric. As the temperature increases, the overall signal decreases[24] as 1/T and the two singularities (S_1 and S_2) broaden and shift towards $g \approx 2$. Moreover a new pair of singularities (N_1 and N_2) also emerge and with increasing temperature they increase in strength relative to S_1 and S_2.

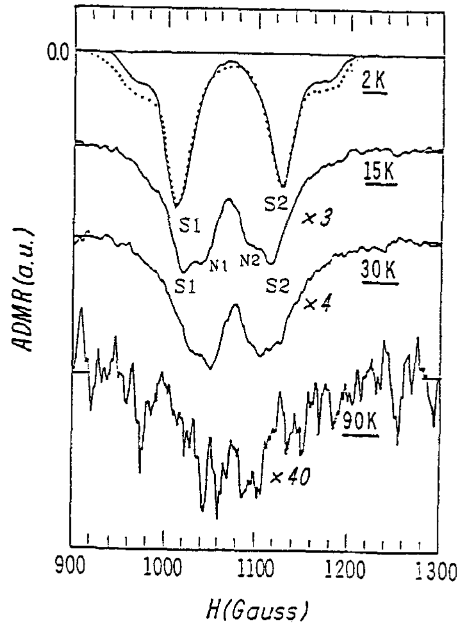

FUGURE 1 ADMR spectra of C_{60}:PS glass at various temperatures.

Recent calculations of JT distortions in C_{60} anion[4-5] have found that the JT energy is about 40 meV and the JT potential surface contains 6 equivalent D_{5d} minima, 10 equivalent D_{3d} maxima, and 15 equivalent D_{2h} saddle points. The JT distortion energy in the lowest excited singlet (neutral) state of C_{60} has been calculated[6] to be about 0.4 eV. Although no calculations have been made on the spin triplet excited state, we can speculate that the JT energy is about that of the singlet state (~0.4 eV), which is higher than all the phonon energies in C_{60} (0.02-0.2 eV). This puts the JT problem in the strong coupling regime ($E_{JT} > E_{phonon}$)[25]. Dynamic JT effects in this regime include pseudorotation, hindered pseudorotation and tunneling splitting, depending upon the barrier energy between the minima in the JT potential surface. The energy levels in the case of pseudorotation in the E⊗ε problem is given as[25]:

$$E_{nm} = \hbar\omega_E(n+1/2) + m^2(\hbar\omega_E)^2/(4E_{JT}) - E_{JT}, \qquad (1)$$

where $\hbar\omega_E$ is the energy of the coupled phonon, n (= 0, 1, 2, ...) is the vibronic quantum number, and m (= ±1/2, ±3/2, ±5/2, ...) is the roton quantum number. We assume that the two types of triplet ADMR powder patterns found in C_{60}:PS glass at T > 4 K are due to the photogenerated triplets which are at the two lowest energy levels in Equation (1), subject to pseudorotation. We then fit the data between 8 K and 35 K with these two types of triplets having different ZFS parameters; one (T_1) with $D_1 = 114\times10^{-4}$ cm^{-1} and $E_1 = 0$; and the other (T_2) with $D_2 = 59\times10^{-4}$ cm^{-1} and $E_2 = 0$. In our calculation we used the density matrix equation method proposed by Alexander[26], Kaplan[27], and Norris et al[28] to calculate the triplet powder pattern under different pseudorotation rates. The resultant powder patterns of the two respective triplets are added with different relative weights. The weights are calculated using a Boltzmann distribution of a two-level system with an energy difference ΔE of ~13±4 cm^{-1} that fits best the data in Figure 1. Also from the fitting we found that the psedorotation rate of T_1 can be expressed as a constant term plus a thermal activation term with an activation energy of ~17±5 cm^{-1}, which is within the uncertainty of the ΔE. The scenario of the spin dynamics in C_{60} is therefore as follows: At 2 K only T_1 is populated, which is subject to a free pseudorotation rate; At higher temperature, T_2 becomes populated and this thermal transition enhances the effective pseudorotation rate for T_1. From Equation (1), the energy difference of the two lowest levels is $2(\hbar\omega_E)^2/(4E_{JT}) = \Delta E \sim 13$ cm^{-1}, and from $E_{JT} \sim 0.4$ eV, we estimate a coupled phonon energy of ~ 300 cm^{-1}.

Figure 2 shows two ADMR spectra of C_{70}:PS at 4 K; they are quite different from the respective ADMR spectrum of C_{60}:PS at 4 K. The H-ADMR spectra show a sharp g≈2 component and a broad pyramid-like triplet powder pattern. We found that they stay the same when measured at different probe energies[29], therefore we speculate that the g ≈ 2 signal is also due to the triplet excitations. As shown in Figure 2, the sharp g ≈ 2 component, however, has a different microwave power dependence; it saturates at a higher microwave power, indicating that it is associated with a spin 1/2 specie. To explain the above discrepancy, we conjecture that the spin 1/2 species are related to the existing radicals in the sample, which interact with the triplet excitons by influencing their recombination rates. To justify this, we measured the dark ESR signal of fresh C_{70} powder and indeed found that there are spin 1/2 radicals with a density N_S of 10^{17} spins/cm^3. For comparison, we note that even in a good a-Si:H sample with N_S

< 10^{16} spins/cm^3, photoexcitations are strongly affected by the spin 1/2 defects[30]. We note that spin 1/2 ADMR signal was not observed in C_{60}:PS (see Figure 1) and this may be due to a lower N_S. We indeed found that in C_{60} N_S is 4×10^{15} spins/cm^3, a factor of 30 smaller than N_S in C_{70} powder. We suspect that the lower spin density in C_{60} is due to that C_{60} is the first product extracted during the fullerene purification process and thus more radicals left in the solution lead to higher spin density in C_{70}.

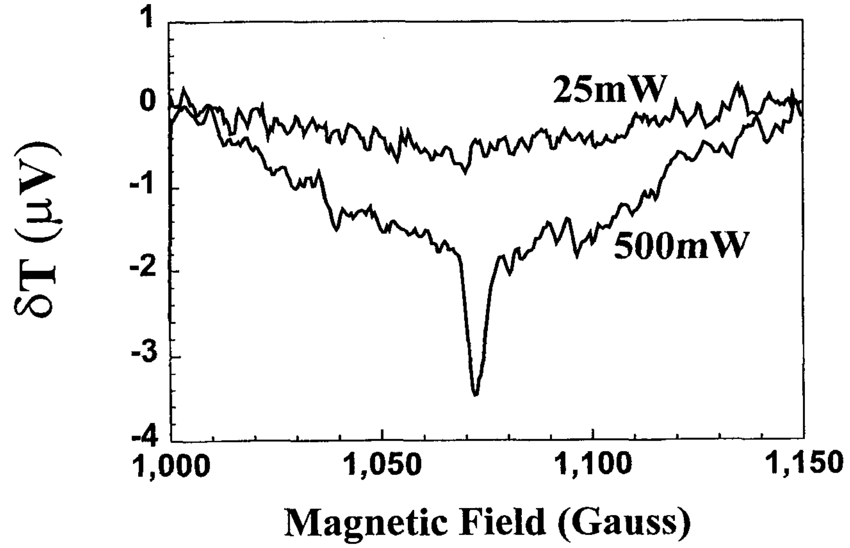

FUGURE 2 ADMR spectra of C_{70}:PS glass at 4 K, measured with high (500 mW) and low (25 mW) microwave powers, respectively.

To fit the curious pyramid-like triplet powder pattern, which does not have any pronounced singularities usually appearing at ±D, ±(D+3E)/2 and ±(D-3E)/2, respectively, around H_0[31], we assume a distribution of triplet ZFS parameters with D ranging upto 55×10^{-4} cm^{-1}, and E = 0. Such a distribution of the ZFS parameters in C_{70} sample was supported by our observation that D is smaller for longer-lived triplets[29].

Figures 3 and 4 show three typical ADMR spectra of sublimed C_{60} and C_{70} films, respectively, measured at different probe photon energies. Each H-dependent ADMR spectrum contains two components with opposite signs and different photon energy spectrum: a broad (powder pattern) component with $\delta n < 0$ and a narrow component at $g \approx 2$ with $\delta n > 0$. Correlated with the broad component, centered at H = 1071 Gauss, there is a δn < 0 "half field" signal at 531 Gauss (not shown here). Based on this and similarity of the powder pattern width to the respective ADMR spectra in C_{60}:PS and C_{70}:PS glass, we identify the negative ADMR component at full and half fields as $\Delta m_s = \pm 1$ and $\Delta m_s = \pm 2$ transitions, respectively, associated with triplet excitons. The explanation for the narrow component at $g \approx 2$ with $\delta n > 0$ is not as straightforward. One possibility is that it is also due to existing radicals in the film, similar as in the C_{70}:PS. However, in that case we observed a $\delta n < 0$ signal (Figure 2), which has the same probe photon energy dependence as that of the triplet powder pattern. Since the wavelength dependence of the spin 1 and spin 1/2 ADMR signals are different here (Figures 3, 4), we identify the narrow positive ADMR component at 1071 Gauss, as due to spin 1/2 photoexcitations with $g \approx 2$. We therefore concluded that the spin 1/2 photoexcitations in sublimed films are associated with charge carriers, probably spin 1/2 polarons ($C_{60}^{\mp}$ or $C_{70}^{\mp}$).

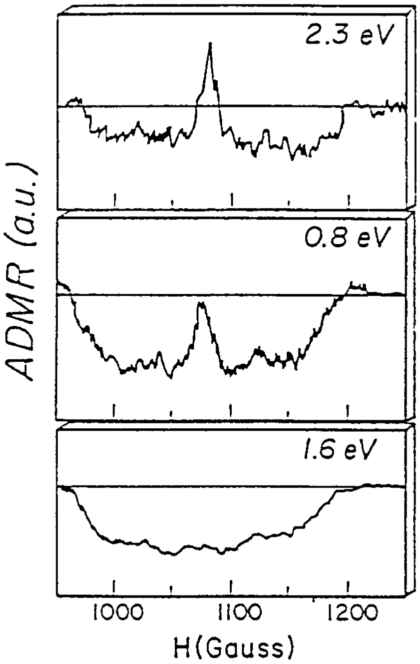

FUGURE 3 Three typical ADMR spectra of C_{60} film at 4 K, measured at various probe photon energies.

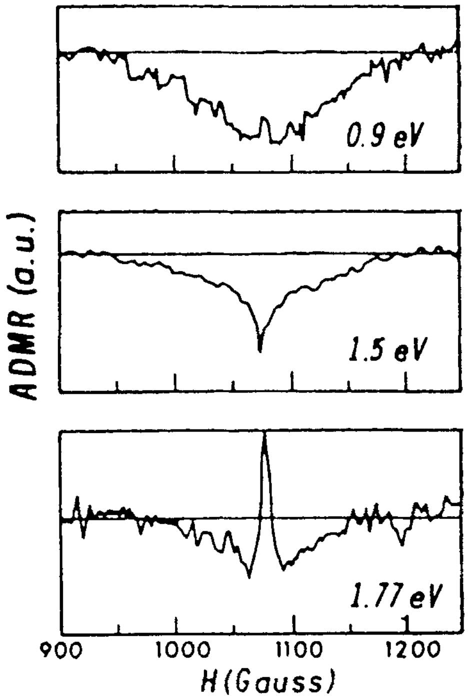

FUGURE 4 Three typical ADMR spectra of C_{70} film at 4 K, measured at various probe photon energies.

SUMMARY

In C_{60}:PS glass, two spin triplet powder patterns were observed, with zero-field-parameter (ZFS), $D_1 = 114\times10^{-4}$ cm^{-1} and $E_1 = 0$; and $D_2 = 59\times10^{-4}$ cm^{-1} and $E_2 = 0$, respectively. Both powder patterns collapse toward the central $g \approx 2$ magnetic resonance line with increasing temperature. We fit the results with a model that relates the two observed triplets with two Jahn-Teller distortion levels, respectively, subject to a temperature dependent pseudo rotation dynamics. The triplet powder pattern in C_{70}:PS glass is pyramid-like with onsets at $H_0 \pm D$ (where $D = 54\times10^{-4}$ cm^{-1}). This shape is different from normal triplet powder pattern and we interpret it with a distribution of ZFS parameters. In sublimed C_{60} and C_{70} films, in addition to the triplet excitations with $\delta n < 0$, we found a spin 1/2 enhancing ($\delta n > 0$) ADMR signal. Compared to the triplet excitations, it has a different wavelength dependent ADMR spectrum. We explain this feature as due to charge separation which uniquely occurs in sublimed films with excitation above the respective C_{60} and C_{70} energy gap.

ACKNOWLEDGMENTS

We thank F. Wudl, V. Srdanov and D. Moses for the fullerene samples used at the start of this work and A. Auerbach for sending us his papers prior to publication. The work was supported in part by the DOE grant no. DE-FG 03-93 ER 45490 and by NSF grant no. DMR-92-22947.

REFERENCE

1. W. Krätschmer, L. D. Lamb, K. Fostriopoulos and D. R. Huffman, **Nature** 347 354 (1990).
2. H. A. Jahn and E. Teller, **Proc. Roy. Soc. A,** 161 220 (1937); C. A. Mead and D. G. Truhlar, **J. Chem. Phys.,** 70 2284 (1979), and references therein.
3. N. Koga and K. Morokuma, **Chem. Phys. Lett.** 196 191 (1992).
4. C. M. Varma, J. Zaanen and K. Raghavachari, **Science** 254 989 (1991).
5. M. Schluter, M. Lanoo, M. Needles, G. A. Baraff and D. Tomanek, **Phys. Rev. Lett.** 68 526 (1991); M. Lanoo, G. A. Baraff, M. Schluter, and D. Tomanek, **Phys. Rev. B** 44 12106 (1992).
6. S. Suzuki, D. Inomata, N. Sashide and K. Nakao, **Phys. Rev. B** 48 14165 (1993).
7. A. Auerbach, N. Manini and E. Tosatti, to be published.
8. M. R. Wasielewski, M. P. O'Neil, K. R. Lykke, M. J. Pellin and D. M. Gruen, **J. Am. Chem. Soc.** 113 2774 (1991).
9. P. A. Lane, L. S. Swanson, Q. X. Ni, J. Shinar, J. P. Engel, T. J. Barton and L. Jones, **Phys. Rev. Lett.** 68 887 (1992).
10. X. Wei, Z.V. Vardeny, D. Moses, V.I. Srdanov and F. Wudl, **Synthetic Metals, 54** 273 (1993).
11. G. L. Closs, et al., **J. Phys. Chem.** 96 5228 (1992).
12. A. Regev, D. Gamliel, V. Meiklyar, S. Michaeli, H. Levanon, **J. Phys. Chem.** 97 3671 (1993).
13. R. W. Lof, et al., **Phys. Rev. Lett.** 68 3924 (1992).
14. S. L. Ren, et al., **Appl. Phys. Lett.** 59 2678 (1991).
15. S. L. Ren, et al., **Appl. Phys. Lett.** 61 124 (1992).
16. M. Matus, H. Kuzmany and E. Sohmen, **Phys. Rev. Lett.** 68 2822 (1992).

17. J. Mort, et al., **Chem. Phys. Lett.** **186** 281 (1991).
18. C. H. Lee, G. Yu, D. Moses, V.I. Srdanov, X. Wei and Z.V. Vardeny, **Physical Review, B** **48** 8506 (1993).
19. H. Yonehara and C. Pac, **Appl. Phys. Lett.** **61** 575 (1992).
20. J. Mort, M. Machonkin, R. Ziolo, and I. Chen, **Appl. Phys. Lett.** **61** 1829 (1992).
21. X. Wei, B. C. Hess, Z. V. Vardeny, and F. Wudl, **Phys. Rev. Lett.** **68** 666 (1992).
22. Y. Kajii, T. Nakagawa, S. Suzuki, Y. Achiba, K. Obi and K. Shibuya, **Chem. Phys. Lett.** **181** 100 (1991).
23. T. W. Ebbesen, K. Tanigaki and S. Kuroshima, **Chem. Phys. Lett.** **181** 501 (1991).
24. X. Wei, Ph.D thesis, University of Utah, 1992 (unpublished).
25 I. B. Bersuker, *The Jahn-Teller Effect and Vibronic Interactions in Modern Chemistry*, Plenum Press, New York (1984).
26. S. Alexander, **J. Chem. Phys.** 37 967, 974 (1962).
27. J. J. Kaplan, **J. Chem. Phys.** **28** 278 (1958); **29** 462 (1958).
28. J. R. Norris and S. I. Weissman, **J. Phys. Chem.** **73** 3119 (1969).
29. X. Wei, S. Jeglinski, O. Paredes, Z.V. Vardeny, D. Moses, V.I. Srdanov, G.D. Stucky, K.C. Khemani and F. Wudl, **Solid State Comm.,** **85** 455 (1993).
30. H. A. Stoddart, Z. V. Vardeny and J. Tauc, **Physical Review,** **38** 1362 (1988), and references therein.
31. J. E. Wertz and J. R. Bolton, *Electron Spin Resonance*, Chapman and Hall, New York (1986).